Detecting Transits of Planetary Companions to Giant Stars

R.J. Assef[1], B.S. Gaudi and K.Z. Stanek

Department of Astronomy, The Ohio State University, 140 W. 18th Ave., Columbus, OH 43210

ABSTRACT

Of the approximately 350 extrasolar planets currently known, of order 10% orbit evolved stars with radii $R_* \gtrsim 2.5R_\odot$. These planets are of particular interest because they tend to orbit more massive hosts, and have been subjected to variable stellar insolation over their recent histories as their primaries evolved off the main sequence. Unfortunately, we have limited information about the physical properties of these planets, as they were all detected by the radial velocity method and none have been observed to transit. Here we evaluate the prospects for detecting transits of planetary companions to giant stars. We show that several of the known systems have a priori transit probabilities of $\gtrsim 10\%$, and about one transiting system is expected for the sample of host stars with $R_* \geq 2.5R_\odot$. Although the transits are expected to have very small amplitudes ($\sim$ few $\times 10^{-4}$) and long durations ($\gtrsim$ 50hrs), we argue that the difficulty with detecting these signals in broadband light is one of systematic errors and practicality rather than photon noise, even for modest aperture ($\sim$ 1 m) telescopes. We propose a novel method that may overcome these difficulties, which uses narrow-band measurements to isolate the thin ring of chromospheric emission expected at the limb of giant stars. The transit signals in these narrow bands are expected to be larger in magnitude and briefer in duration than in broad-band emission, and thus alleviating many of the difficulties with transit detection in broad-band emission. Finally, we point out that it may be possible to discover planetary companions to giant stars using Kepler, provided that a sufficient number of such targets are monitored.

Subject headings: planetary systems – stars: variables: other – techniques: photometric

[1]e-mail: rjassef@astronomy.ohio-state.edu

1. Introduction

Since the first extrasolar planet orbiting a main-sequence star was detected by Mayor & Queloz (1995), the number of known planets has increased very rapidly. To date we know of about 300 exoplanets in the local solar neighborhood. Most of these were detected via the radial velocity (RV) variations they induce on their host star, and the typical hosts of these planets are F, G and K main sequence stars. This is illustrated in Figure 1, which shows a color-magnitude diagram of stars with planets originally detected with RV.

Among this sample of planets are a class of Jovian-mass ($\sim 0.1 M_J$ to a few M_J) planets with periods of $\lesssim 10$ days. These "Hot Jupiters" were quite unexpected in the standard core-accretion planet formation model, which was developed to explain the solar system, and set the expectations for extrasolar planets (Lissauer 1987). The environmental conditions and evolutionary history of these planets are quite distinct from that of the giant planets in our solar system. In particular, the energy budget of hot Jupiters is dominated by the immense stellar isolation flux they receive, which is a factor of $\sim 10^4$ higher than that for Jupiter, and a factor of $\sim 10^4$ higher than the cooling flux of an isolated planet after a few gigayears. This large stellar insolation has a profound effect on the properties of these planets. In particular, their outer atmospheres develop a deep, isothermal layer above the convective zone and below the photosphere, which slows the rate at which the planet cools. If these hot Jupiters migrated to their present, high stellar insolation environment on a timescale that is short compared to their cooling time in isolation of $\sim 10^6 - 10^7$ yrs, then their rate of cooling and hence contraction will be significantly slowed. As a result, hot Jupiters are predicted to be significantly larger than Jupiter at their current ages of a few Gyr. At fixed mass and composition, their radii are predicted to be correlated with their equilibrium temperatures (T_{eq}). Jovian-mass planets orbiting solar-type stars beyond ~ 0.1 AU are hence predicted to have smaller radii than hot Jupiters, although still slightly inflated with respect to planets with $a \gtrsim 1$ AU (Fortney et al. 2007). In contrast, super-Jupiter planets more massive than a few M_J will have higher surface gravities, are expected to contract more quickly than Jovian-mass planets, and are more nearly purely degenerate. Therefore, their radii are expected to be much less sensitive to their age (for ages $\gtrsim 10^8$ yrs), composition, or the amount of stellar insolation they receive (Guillot 2005).

Transiting planets offer the possibility of precision tests of these theoretical predictions. With a combination of radial velocity measurements, stellar spectra, and precise photometry of the planetary transit, it is possible to infer the radii, mass, and equilibrium temperatures of transiting planets to an accuracy of a few percent (e.g., Torres et al. 2008). These measurements can be directly compared with detailed theoretical model predictions (Burrows et al. 2000; Hubbard et al. 2001; Burrows et al. 2003; Bodenheimer et al. 2003;

Laughlin et al. 2005), although such comparisons must allow for unknown or poorly constrained parameters, such as the mass in heavy elements, and the age of the star. These comparisons generally verify the most basic prediction of these models, namely that the radii of hot Jupiters should be inflated with respect to similar planets in isolation (Burrows et al. 2000; Laughlin et al. 2005). However, there are significant discrepancies as well, and in particular a significant fraction of the known transiting planets have radii that are far too large to be explained by the simplest models, even including the effects of stellar irradiation. This is a long-standing problem (Burrows et al. 2003), and although many solutions have been proposed (Bodenheimer et al. 2003; Guillot & Showman 2002; Winn & Holman 2005; Burrows et al. 2007; Mardling 2007; Jackson et al. 2008), no consensus has yet emerged as to the correct explanation.

Precise radii of planets over a wider range of physical and environmental conditions would, in principle, provide more decisive tests of these models, and may even shed light on the origin of the anomalously large radii. Unfortunately, photometric transit surveys, which have discovered the majority of transiting planet systems, are strongly biased toward short-period systems (Gaudi et al. 2005). Furthermore, these surveys are sensitive to the transiting planets orbiting main-sequence stars with apparent magnitudes of $V = 10 - 13$, which are dominated by F and G dwarfs (Pepper et al. 2003). As a result, the majority of known transiting planets occupy a fairly narrow region of parameter space, namely semimajor axes of $\lesssim 0.1$ AU and main-sequence hosts with $0.7M_\odot \lesssim M \lesssim 1.5M_\odot$. Radial velocity surveys are less strongly biased with respect to semi-major axis than transit surveys, and indeed the transiting planet with the lowest-mass host, and the transiting planet with the largest semi-major axis, were both first discovered by RV (Butler et al. 2004; Fischer et al. 2007), and subsequently shown to be transiting (Gillon et al. 2007; Barbieri et al. 2007). Follow-up searches for additional transiting systems among the sample of known planets detected by RV (Seagroves et al. 2003) may uncover some with long periods and thus considerably expand the parameter space over which giant planet models are tested. Space-based transit missions are also less biased with respect to semi-major axis, and should detect many long-period transiting planet systems (Beatty & Gaudi 2008; Yee & Gaudi 2008).

While the majority of the nearby exoplanet hosts are main-sequence FGK stars with masses of $0.7M_\odot \lesssim M \lesssim 1.5M_\odot$ and radii of $0.7R_\odot \lesssim R_* \lesssim 2.5\ R_\odot$, roughly $\sim 10\%$ are evolved stars with $R_* \gtrsim 2.5\ R_\odot$. These giant stars are interesting targets for planet searches because they tend to have main-sequence progenitors that are earlier spectral type and so more massive than exoplanet hosts on the main-sequence. As both the mass of the protoplanetary disk and the dynamical time at the location of the snow line are expected to depend on the mass of the primary, it is a generic prediction that the mass and/or frequency of giant planets should depend on the mass of the primary (Ida & Lin 2005;

Kennedy & Kenyon 2008). Searching for planets orbiting main-sequence stars much earlier than spectral type F5 ($M \gtrsim 1.5\ M_{\odot}$) is challenging due to the fact that these stars are hot and thus have few spectral lines in the visible. Furthermore, these stars tend to be fast rotators, and thus what spectral lines are available tend to be broad. Although there are RV surveys that target these stars (Galland et al. 2005), they are generally only sensitive to massive, super-Jupiters and brown dwarf companions (Galland et al. 2006). When these stars evolve off the main-sequence, however, they expand and cool, thus making them much more amenable to RV surveys (Sato et al. 2003; Johnson et al. 2007a).

To date, $\sim$ 25 planetary companions to nearby stars with $M > 1.5\ M_{\odot}$ have been discovered. Four correspond to planets orbiting main-sequence A stars detected by direct imaging, namely Fomahault b (Kalas et al. 2008) and HR 8799 b, c and d (Marois et al. 2008), while the rest of the hosts are exclusively evolved stars with $R_{*} \gtrsim 2.5 R_{\odot}$. Planetary companions to giant stars offer the possibility of testing models of the structure and atmosphere of giant planets for a relatively unique set of physical parameters and under a relatively unique set of environmental conditions. Consider, for example, a $M_p \sim 3\ M_J$ companion with a semimajor axis of $a \simeq 1$ AU orbiting an intermediate mass main-sequence A star with $M \sim 2.0\ M_{\odot}$. If we assume that this planet formed *in situ*, or migrated to this location on a timescale less than its cooling time of $\lesssim 10^7$ years, it would have cooled in the presence of a stellar insolation flux that is a factor of ~ 40 times smaller than a typical hot Jupiter companion to a $\sim M_{\odot}$ star. Since the cooling time of the planet is significantly shorter than the main-sequence lifetime of the host, it is expected that the planet will cool and contract to a radius $\sim 1.1\ R_J$ (Fortney et al. 2007) before the host star leaves the main sequence. Figure 2 shows the evolution of such a host after it leaves the main sequence, according to the Padova stellar evolution tracks from Salasnich et al. (2000). The luminosity at first decreases slightly as it approaches the base of the giant branch, and then begins to rise as the star ascends the giant branch. Over the next $\sim$ 20 Myr, the luminosity of the host increases by a factor of ~ 10, while the radius increases by a factor of ~ 5. Thus the insolation flux of the planetary companion increases by factor of ~ 10, corresponding to an increase in the equilibrium temperature of the planet of ~ 400 K[2]. At the tip of the giant branch, the planet will have $T_{eq} \sim 1000$ K, similar to that of hot-Jupiter companions to solar-type stars with $a \sim 0.1$ AU.

As a result of the change in insolation, the atmospheric scale height H of the planet will increase on a thermal timescale of $\sim 10^2 - 10^4$ years (Showman et al. 2008), which is

[2]Here we have assumed, for simplicity, that all of the incident stellar radiation on the planet is absorbed and re-emitted isotropically, and that these characteristics, as well as the planet semimajor axis, do not evolve with time.

essentially instantaneous compared to the timescale of changes in the insolation flux. Note that the bulk of the planet is not expected to be affected, as the planet has already cooled, and the external heating cannot go against the entropy gradient (Burrows et al. 2000). Thus it is expected that the changes in the stellar insolation will only affect the outer scale height H of the atmosphere, and thus the overall change in the planet radius will be due only to the changes in H. The scale height H will correlate linearly with equilibrium temperature for a simple, isothermal atmosphere, such that

$$H = \frac{kT_{eq}}{\mu m_p g},$$

where μ is the mean molecular weight, g is the surface gravity, and m_p is the proton mass. Accounting for the transit radius effect (e.g., Burrows et al. 2007), changes in H will then result in changes in the apparent radius of a transiting planet of

$$\frac{\Delta R_p}{R_p} \simeq \frac{H}{2R_p} \ln \frac{2\pi R_p}{H}.$$

For this particular case, it is expected that the radius of the planet will only increase by $\sim 0.1\%$ relative to its radius when the host was on the main-sequence (Fig. 2). This is unlikely to be detectable. However, for planets with lower surface gravities, the effect will be larger and potentially detectable.

The basic prediction is therefore that the radii of the known planetary companions to giant stars will have been largely unaffected by the post main-sequence evolution of their hosts. Nevertheless, it would be quite interesting to test this prediction. Furthermore, the existence of the heretofore unexplained population of 'bloated planets' with radii larger than predicted by models suggests that this prediction may not be entirely robust. In particular, if, as suggested by Guillot & Showman (2002), the bloated radii can be explained by a small fraction of the stellar insolation energy being deposited deep in the interiors of the planets through winds in the atmospheres, then the large changes in the stellar isolation flux experienced by planetary companions to evolved stellar hosts could lead to significant changes in their radii. Since the transit depth is proportional to the square of the radius of the planet, this would have important implications for their detectability. Other observable effects of the change in stellar insolation are also possible, such as an increase in the atmospheric evaporation rate (Baraffe et al. 2004; Hubbard et al. 2007).

Thus it would be of considerable interest to detect transiting planetary companions to evolved stars, in order to measure their radii and so test models of the structure, evolution, and atmospheres of these planets. Unfortunately, all of the planetary companions to giant stars have been found by RV surveys and none of them have been observed in transit, so

our knowledge of them is very limited. In this paper we discuss the possibility of detecting transits of the known planets orbiting giant stars. In § 2 we discuss the probability of seeing one of these planets transiting its parent star, while in § 3 we address the difficulties and prospects of detecting them. In §§ 4 and 5 we present a novel technique for observing planetary transits in giant stars by using narrow-band filters that could potentially overcome all the difficulties inherent in their broad-band signals.

2. Transit Probability

As summarized previously, several tens of planets orbiting giant stars have been discovered by radial velocity surveys, but to date none has been observed to transit its parent star. Indeed, to the best of our knowledge, no attempt has been made to search for transits among the known planetary companions to giants. This is likely due to the dauntingly small expected signal, and the difficulties in detecting such small signals from ground-based observations. We discuss these issues further in the next section. Nevertheless, there is a significant probability that one of these planets should be transiting as seen from Earth. The a priori probability that a planet will transit is given by (e.g. Seagroves et al. 2003)

$$P_{\rm tr} \;=\; 0.0045 \left(\frac{1{\rm AU}}{a}\right) \left(\frac{R_* + R_p}{R_\odot}\right) \left[\frac{1 + e\cos(\frac{\pi}{2} - \varpi)}{1 - e^2}\right], \qquad (1)$$

where a is the semi-major axis of the orbit, R_* and R_p are respectively the star's and planet's radius, e the eccentricity of the orbit and ϖ the longitude of periastron. The probability of transit is directly proportional to the star's radius but inversely proportional to the semi-major axis of the planet. Thus it is not immediately obvious whether the probability is higher or lower for the planetary companions to giant stars as compared to typical transiting hot Jupiters, as the larger radii of the giant hosts compensate for the larger typical separation of their planetary companions (see Sato et al. 2008). To estimate the number of known planets around giant stars we would expect to observe in transit, we obtain the public list of known planets found by RV surveys as compiled by *The Extrasolar Planets Encyclopedia*[3]. We first consider all types of stellar hosts. To estimate the transit probability for each system, we obtain a, e, ϖ, R_* and R_p from this list whenever possible. If R_p is not listed, we assume the planet to be of Jupiter size. If R_* is not listed, we estimate it from the angular size – color relations of van Belle (1999) and parallax from Hipparcos (Perryman et al. 1997). The angular size – color relation is different for main sequence and evolved stars, which poses a problem since we generally do not have a priori information of the luminosity class of the

[3]http://exoplanet.eu/ as of October 10$^{\rm th}$, 2008

objects. We assume that a given star is on the main sequence unless the determined radius is larger than $1R_\odot$ (which is roughly the local turn off radius), in which case we recalculate it with the relation for evolved stars. Recently, these calibrations have been revised by van Belle & von Braun (2009) but we have not updated our calculations as the changes are not too significant for the relevant objects. For all stars we obtain V band photometry from SIMBAD[4], and K band photometry from the Two Micron All Sky Survey (2MASS) All-Sky Catalog of Point Sources (Cutri et al. 2003) via the Vizier service[5]. Five exceptions to this process must be noted. (1) We eliminate TW Hya b from our sample because its existence has recently been questioned by Huelamo et al. (2008). (2) We correct the radius of the star HD13189 to that measured by Baines et al. (2008), from the value listed by *The Extrasolar Planets Encyclopedia*, which is 100 times larger. (3) We correct the V-band magnitude of the M Dwarf GJ317, as SIMBAD lists it to be 1 magnitude fainter than what is commonly quoted (Johnson et al. 2007b). (4) The B- and V-band magnitudes of HD330075 are corrected to the values reported by Pepe at al. (2004), which are about 0.3 magnitudes fainter in both bands than the values listed by SIMBAD. (5) For HD47536b, no value for the semi-major axis is listed in the *The Extrasolar Planets Encyclopedia*, and so we estimate a=1.5AU based on the mass of the primary determined by Setiawan et al. (2008) and the orbital period determined by Setiawan et al. (2003). The color magnitude diagram of all the host stars in our sample is shown in Figure 1, together with all the sources in the Hipparcos catalog. It is clear that most exoplanet hosts are main-sequence stars with $0.4 \lesssim B-V \lesssim 1$. About 13% of hosts are evolved stars with $R_* \gtrsim 2.5R_\odot$. The majority of these are red clump stars. The largest exoplanet host star is HD13189 with a radius $\sim 50\ R_\odot$, which has a $M_p \simeq 14\ M_J$ companion at a separation of $a \simeq 1.85$ AU.

Figure 3 shows the transit probability and semi-major axis as a function of the radius of the host star for the systems in our sample. For main sequence stars, $\log a$ and thus the transit probabilities appear to be roughly distributed uniformly for $a \gtrsim 0.04$ AU. For evolved hosts with $R_* \gtrsim 2.5R_\odot$, however, no system has a semi-major axis smaller than $0.61AU$ (Niedzielski et al. 2008; Sato et al. 2008). There are four systems that have a priori transit probabilities greater than 10%. These are 4UMa b ($P_{\rm tr} \simeq 0.15$), HD122430 b ($P_{\rm tr} \simeq 0.32$), HD13189 b ($P_{\rm tr} \simeq 0.15$) and HIP75458 b ($P_{\rm tr} \simeq 0.17$). These may be the best targets to search for transiting companions, although they are also expected to have the smallest transit signals, with depths of $2.55 \times 10^{-5}, 2.01 \times 10^{-5}, 4.16 \times 10^{-6}$, and 5.80×10^{-5}, respectively, for a companion with $R_p = R_J$.

[4]http://simbad.u-strasbg.fr/simbad/

[5]http://vizier.u-strasbg.fr/

Figure 4 shows the number of planets detected by RV surveys that we expect to be transiting, as a function of the minimum stellar radius of the hosts. If we consider only planets orbiting stars larger than $2.5R_{\odot}$, we expect about one to be transiting.

3. Detecting Planets Around Giant Stars

In the previous section we demonstrated that we expect of order one transiting companion among the exoplanet host stars with radii larger than $2.5R_{\odot}$. Despite this, to the best of our knowledge, no follow up observations are being conducted to search for these transits.

Nominally, the signal to noise ratio (S/N) for the transit of a planet in front of a giant star can be very large. Consider, as a fiducial example, a planet with $R_p = R_J$ orbiting a red giant star with mass $M_* = 1M_{\odot}$ and radius $R_* = 5R_{\odot}$. These values are typical of red giants in the solar vicinity. Recently, Sato et al. (2008) found that planetary companions to giant stars with intermediate-mass ($1.7 < M < 3.9M_{\odot}$) main-sequence progenitors appear to have a minimum semi-major-axis of 0.68AU. Since, at fixed R_*, the closest planets will have the highest transit probability, we will therefore assume for our fiducial case $a = 0.7$AU. In the absence of correlated noise, the S/N of a transit is

$$\frac{S}{N} \sim n^{1/2} \frac{\delta}{\sigma}, \tag{2}$$

where n is the number of data points during transit, δ is the fractional transit depth, and σ is the fractional photometric precision. If photons are collected at a rate Γ, and the transit duration is t_T, then

$$\frac{S}{N} \sim \sqrt{\Gamma t_T}\, \delta. \tag{3}$$

For our example case

$$\delta = \left(\frac{R_p}{R_*}\right)^2 \approx 4 \times 10^{-4} \left(\frac{R_p}{R_J}\right)^2 \left(\frac{R_*}{5R_{\odot}}\right)^{-2}, \tag{4}$$

where R_J is the radius of Jupiter, and the transit duration is

$$t_T \approx 54 \text{ hours} \left(\frac{a}{0.7\text{AU}}\right)^{1/2} \left(\frac{R_*}{5R_{\odot}}\right) \left(\frac{M}{M_{\odot}}\right)^{-1/2}, \tag{5}$$

where we have assumed a circular orbit for simplicity. The average V-magnitude of the exoplanet hosts with $R_* > 2.5R_{\odot}$ is $V = 5.5$. If we assume a telescope with a 1m aperture with and overall efficiency of 50% (i.e., we detect 50% of the photons from the star), the S/N of our example case would be ~ 870 per transit.

Even though this nominal value for the S/N ratio is extremely large, it must be taken into account that the transit duration t_T is long enough that such a transit cannot be observed from a single facility unless it is located in space. In practice, a ground-based telescope would only be able to observe a small part of the transit, significantly degrading the signal to noise ratio. If neither ingress or egress are observed, the photometry is unlikely to be sufficiently stable from night-to-night to identify transits of such small depths.

Even if the difficulties posed by the long transit duration could be overcome by, for example, a network of telescopes around the world with properly accounted photometric offsets, the transit might still be very hard to detect because of correlated errors in the relative photometry, commonly known as "red noise." It is unclear what exactly causes this noise, but it is most likely a combination of effects including seeing variations, airmass changes and flatfielding errors. These correlations introduce coherent modulations in the light curves that can corrupt the transit signal (see Pont et al. 2006 for a detailed discussion). In current photometric transit surveys, the typical level of the red noise is of the order of 10^{-3} magnitudes and is thought to be correlated in timescales of a few hours (Gould et al. 2006; Pont et al. 2007). Since the transit signal of a Jupiter-sized planet around a giant star is significantly smaller than this (for our fiducial case it is $\sim 4 \times 10^{-4}$ magnitudes) current transit surveys are unable to detect transiting Jupiter-sized planets around giant stars, although it should be kept in mind that it is generally not known how red noise behaves on the timescales relevant for this problem. Errors are known to be less correlated between consecutive nights, therefore it might be the case that the very long duration of planetary transits of giant stars mitigates the effect of the red noise.

Targeted photometric follow-up of transits in bright stars can achieve very low levels of systematic noise even when the observations are taken from the ground, as controlling the possible causes of red noise is much simpler when all efforts are concentrated on a single system. For example, Winn, Holman & Roussanova (2007) performed ground-based photometric follow-up observations of the planetary system TrES-1 (Alonso et al. 2004) and were able to reduce the correlated errors in short timescale observations ($\sim$ 3 hours) to a level smaller than 10^{-4} magnitudes. See also Johnson et al. (2009) and Winn et al. (2009). Nutzman et al. (2008) observed transits of HD149026b from space with the 8μm channel of IRAC on Spitzer and controlled the systematic errors to a very similar level on longer timescales ($\sim$ 7 hours). While the regimes in which these observations have been made do not necessary apply to planetary transits in giant stars, their precision is very encouraging and suggest that, in the near future, transit follow-up observations of known planets around giants could achieve the photometric precision and control of systematics necessary to detect transiting Jupiter-size companions. Nevertheless, a note of caution must be drawn, as one of the ways these surveys control systematic errors is by removing long timescale photometric

trends, such as linear changes in the flux over a night or night-to-night average flux variations, as these could be caused by, for example, flatfielding errors. For close-in planets this does not represent a problem, as the transit durations are short compared to the scales over which these trends appear, but the transit durations for planets around giant hosts are considerably longer, and thus their signal could be interpreted as due to systematic errors in the photometry.

With their continuous photometry and better control of systematic errors, space missions like *Kepler* (Borucki et al. 2003) and *COROT* (Baglin et al. 2006) could be very sensitive to Jupiter-sized companions transiting in front of giant stars in their field-of-view, and thus have the potential to discover such systems. Indeed, the depth of the transit of a $\sim R_J$ planet transiting in front of a $\sim 10R_\odot$ star is quite comparable to the transit depth of an Earth-sized planet transiting in front of a solar-type star, precisely the signal that *Kepler* was designed to detect. Furthermore, for planets at $a \sim 1$ AU, the duration of the transit signal is ~ 10 times longer. If we assume that red noise in Kepler is negligible and the S/N can be estimated by means of equation (3), taking the value of Γ listed in Kepler's official website[6] yields $S/N \approx 35$ per transit for $R_* = 5R_\odot$, $R_p = R_J$, $a = 0.7$ AU, and $V = 14$, which is near the faint limit of *Kepler*. The field of view of *Kepler* is estimated to have 223000 stars brighter than $m_{\rm v} = 14$ of which 136000 should be on the main sequence. Most of the 87000 other stars should be red giants, but currently most of them are set to be eliminated before the data is downloaded from the satellite. If only 1000 of them were downloaded, assuming a radius of $R_* = 5R_\odot$ for these stars, and that 5% of them host a Jupiter-sized planet at $a = 1$ AU, the expected number of transiting systems is approximately 1.

All the estimates we have derived here assume that the intrinsic variability on the time-scales relevant to planetary transits is small compared to the depth of the transits. While this is true and very well studied for F, G and K dwarfs, little is known about the variability of giant stars on the time-scales of tens of hours. Baliunas et al. (1981) studied the short time-scale variability of chromospheric CaII of 4 giants (α Boo, α Tau, α Aur and λ And) using high resolution spectra, and for two of them (α Tau and λ And) also using the HKP2 spectrophotometer on the Mount Wilson 60-inch telescope (see § 5.1 for a more detailed description of the instrument). While no variability of the CaII H and K lines was found in the high resolution spectra, the spectrophotometry shows some significant quasi-regular variability of 10% or less on timescales of 8–30 minutes for λ And and of 25–30 minutes for α Tau. Adelman (2001) studied the variability of red clump giants in the Hipparcos database and found most of them to be constant within 0.03 mag. Several studies of this

[6]http://kepler.nasa.gov

type of variability have been done for Mira type variables with extremely discrepant results. Smak & Wing (1979), Maffei & Tosti (1995) and de Laverny et al. (1998) observed short time-scale broad-band variability of Mira variables in the visible and near-IR. In particular, de Laverny et al. (1998) observed 51 variability events of 0.23 to 1.11 mag variations with time-scales of 2 hours to 6 days in a sample of 39 Miras from the Hipparcos catalog. In contrast, Smith et al. (2002) found no short time-scale (hours to days) variability in the near- to mid-IR observations of 38 Mira variables from the COBE DIRBE (Hauser et al. 1998) database. Also, Woźniak, McGowan & Vestrand (2004) failed to detect this effect in a sample of 485 Miras in the Galactic bulge based on I-band observations from the OGLE-II experiment (Udalski, Kubiuak & Szymański 1997). They derive an average upper limit on the rate of irregular rapid-variability events of the type found by de Laverny et al. (1998) of 1 per 26 years per star, in striking contrast to the rate of 1 event per year per star implied by the de Laverny et al. (1998) results. They identify three possible resolutions to this apparent discrepancy: (1) the Mira variables in the Galactic Bulge population differ from their counterparts in the solar neighborhood, (2) the variability is in a part of the spectrum not covered by the Cousins I-band used by OGLE-II, or (3) the short time-scale variability events are much less frequent than suggested by de Laverny et al. (1998). Recently, Aigrain et al. (2009) studied the noise properties of the *COROT* data from its first 14 months of observations and determined that stars identified as likely red giants exhibited a magnitude-independent noise scatter of 0.5 mmag on 2 hour timescales, significantly higher than for stars identified as likely dwarfs. They interpret this increased scatter as intrinsic photometric variability. However, it is not clear how this amplitude of intrinsic variability should be extrapolated to the 50 hr timescale relevant for planetary transits. Kallinger et al. (2008) studied the Fourier spectrum of 31 likely red giants in the *COROT exofield* and found that these stars show a variability of 0.05–0.1 mmag in timescales of 50 hrs ($\sim 5\mu$Hz). This amplitude of variability is of the order of the expected transit depths for giant stars and could significantly hinder the ability to identify them. Without a consistent picture of variability in red giants it is not possible to assess its effects on the detection of planetary transits, although it is very encouraging that several independent studies have found either null results or amplitudes of variability that would not be disastrous for their identification.

While it seems that in the near future detecting transits around giant stars could be possible with current techniques, in the following sections we show that it might also be possible to detect them by using narrow band filters centered on the CaII H and K lines rather than with the commonly used broad-band filters. Observations in these bands may overcome many of the difficulties discussed above, as the transit depths can be much deeper and the transit durations are much shorter.

4. Limb Brightening of Giant Stars

The great majority of the flux from stars comes from their photosphere, where gas is relatively cool compared to the inner regions and elements leave imprints of absorption lines in the light spectrum. Surrounding the photosphere, gas of significantly higher temperature ($\sim 20,000$K) and lower density has been observed in some stars. We call this atmospheric layer the chromosphere and, because of its physical conditions, some resonant transitions that are still optically thick in this region produce emission lines in the spectrum. This means that while for most wavelengths the star will appear to be brighter at the center and fainter towards the limb, at the wavelengths of these transitions the radial surface brightness distribution will have the opposite trend: it will appear as a faint disc surrounded by a brighter limb.

Studying the emission lines coming from the chromosphere and their possible variability can be crucial to understanding the heating mechanisms of this region (either magnetic, mechanic or a combination of both; see e.g. Pasquini, de Medeiros & Girardi 2000) and processes of mass loss in different stars (e.g Dupree, Whitney & Pasquini 1999). A big drawback is that most of these lines fall in the UV part of the spectrum, rendering them unobservable from the ground. This makes the CaII doublet (H and K lines) of particular interest, as it falls directly in the optical region (λ3933 Å and λ3960 Å for H and K respectively) and can exhibit very strong narrow chromospheric emission in stars of types later than F0 (Shkolnik, Walker & Bohlender 2003). In some cases, the emission line is double peaked, exhibiting a centrally reversed profile (e.g. Dupree, Whitney & Pasquini 1999).

While this emission is found in every star that has a chromosphere, it is particularly important in red giant stars as their atmospheres are significantly more extended than those of dwarfs. For example, the Sun has been observed to show resonant line scattering in its limb over a ring of a width of order $0.01R_{\odot}$, while for red giants this width can be 1–2 orders of magnitude larger (see Loeb & Sasselov 1995, and references therein).

Monitoring of the CaII H & K emission in bright stars has been routinely done for the last 30 years (Wilson 1978; Duncan et al. 1991; Wright et al. 2004) and has been recently used as a tool for estimating chromospheric activity and radial velocity jitter in stars targeted by radial velocity surveys for planets (Wright et al. 2004). In the next section we describe a novel technique to observe planetary transits that takes advantage of the limb brightened profile shown by red giant stars at the wavelengths of CaII H & K that may overcome many of the difficulties with detecting transits using broad-band based measurements.

5. Transits in H & K

5.1. Detecting Transits in H & K

As described in the last section, if we were to observe a giant star through narrow band filters centered on the CaII H & K lines, we would see a faint disc surrounded by a brighter ring, in sharp contrast to the more familiar limb-darkened disc seen in broad-band light. As the width of the CaII H & K line emitting region is much smaller than the radius of the star, transiting planets will block a significantly larger fraction of the light than in the uniform disk case. Figure 5 shows how the transit light curve would appear in CaII H & K for the same fiducial case discussed in §3, a Jupiter-sized planet transiting a $5R_{\odot}$ giant star, compared to the uniform disk model assumed before. The depth of the transit is about 8 times larger for the former case and is well above the red noise limit of current surveys when crossing the brightened limb, while during the inner disk transit it is much shallower. For simplicity, in this figure, and for the rest of the section, we have assumed that the star can be modeled as an inner uniform disk surrounded by a ring of width in units of the stellar radius R_* of $w = 0.05$ that has an intensity relative to the inner disk intensity of $I = 30$. Note that R_* refers to the photospheric radius of the star rather than the chromospheric radius. The values of w and I were taken to roughly reproduce the limb brightening model of Loeb & Sasselov (1995) for a $100R_{\odot}$ red giant star. While this model is probably not accurate for the smaller giant stars we consider here, it is sufficient to provide an order of magnitude estimate of the detectability of these types of transits. Below we will describe how the S/N depends on the exact value of these parameters. Proper modeling of the chromospheric emission in giant stars involves extensive non-LTE atmospheric calculations that go beyond the scope of this work.

In this model, the chromospheric transit depth δ_R (i.e. the transit depth when transiting the chromosphere but considering both light components) can be easily described in two limiting cases. When the width of the ring is much smaller than the radius of the transiting planet, the chromospheric transit depth is,

$$\delta_R \;=\; \frac{p}{\pi}\,\left(\frac{2Iw+\pi p/2}{2Iw+1}\right), \qquad (w \ll p), \tag{6}$$

where $p \equiv R_p/R_*$. When the width of the ring is larger than the planet's diameter, the chromospheric depth is

$$\delta_R \;=\; \frac{Ip^2}{Iw(2+w)+1}, \qquad (w > 2p). \tag{7}$$

Note that in the limit where the flux of the chromospheric ring is much greater than that of the disc, equation (6) converges to $\delta_R = p/\pi$, completely independent of the ring's width.

Thus for $w \ll p$, the chromospheric transit depth is larger than the broad-band (photospheric) depth by a factor of $\sim (\pi p)^{-1}$.

It is worth noting that there exist instruments specifically designed to observe the flux in the CaII H & K lines. They are commonly used in conjunction with radial velocity surveys in order to monitor chromospheric activity in the target stars. One such instrument is the HKP-2 (Vaughan, Preston & Wilson 1978) at Mount Wilson. To estimate the S/N of the detection of one of these transits, we will assume that the observations are carried out on the H and K filters of the HKP-2 instrument. Both bands have a triangular instrumental profile with a FWHM of approximately 1 Å centered at the CaII H & K lines respectively. Assuming that the flux per unit wavelength F_λ is the same as at the effective wavelength of the Johnson's B-band, the signal to noise ratio is given approximately by

$$\left(\frac{S}{N}\right)^2 = \left(\frac{2445}{\text{sec.}}\right) eN_T \left(\frac{A_T}{\text{cm}^2}\right) 10^{-0.4m_B} \int_{t_i}^{t_e} \left(\frac{F(t)}{F_{\text{out}}} - 1\right)^2 dt, \tag{8}$$

where N_T is the number of transits observed, e is the total efficiency of the observation (fraction of photons detected), A_T is the effective area of the telescope, m_B is the B-band magnitude of the star, $F(t)$ is the observed flux as a function of time, F_{out} is the star's flux outside transit and t_i and t_e are the times of first and last contact with the chromosphere respectively. For the same fiducial case of §3, assuming $e = 1/2$, we find $S/N \simeq 43$. If we eliminate the inner disk part of the transit, since it is unlikely to be detected, the S/N drops almost negligibly to 42. Note that in equation (8) we have assumed that the S/N is limited by the flux of the source. The noise from the background should be negligible for such a bright star even in these narrow filters. However, as we discuss below, the contribution to the photometric uncertainty from the reference stars may be important. The total transit time is, as before, approximately 55 hours, but each ring crossing (note that there are 2 per transit) takes only 1.2 hours. This fact, coupled with the fact that the transit depth is much larger (by a factor of $\sim (\pi p)^{-1}$) than for a uniform disk, as shown in Figure 5, makes the narrow band transits, in principle, much simpler to detect. Note that if one were not lucky enough to see both ring transits, the S/N would only degrade by a factor of $\sqrt{2}$.

Photometric studies of planetary transits typically rely on precise *relative* photometry in order to control systematic errors. In this technique, the variable star's flux is measured relative to other constant stars in the field. Observations in the narrow bands H and K pose a potential problem for performing relative photometry, as giant stars are so bright and rare that there may not be a sufficient number of reference objects to do a reliable comparison. One way to overcome these difficulties is to measure the Mount Wilson $S-$value, introduced by Duncan et al. (1991). The $S-$value is a self calibrating index based on the H and K filters plus two broader bandpasses: one redwards of H, called R, and one bluewards of

K, called V. Both of these reference bandpasses have a FWHM of 20Å and a rectangular instrumental profile (for details see Duncan et al. 1991; Wright et al. 2004). The $S-$value is then defined as

$$S \;=\; 2.4\,\frac{F_H \;+\; F_K}{F_R \;+\; F_V}, \tag{9}$$

where F_X is the flux observed through band X.

Figure 6 shows the shape of a transit as viewed through the $S-$value. We have assumed the same parameters as for Figure 5. Notice that the ring transit is of equal depth as before and that during the inner disk transit the $S-$value is larger than outside transit, with a magnitude similar to the broad-band transit depth. For the $S-$value, the analytic form of the S/N would be roughly the same as for the narrow band filter transits (eqn. [8]), as the noise is dominated by the H and K bands rather than by the R and V channels. The overall detection S/N for the $S-$value observations of the transit is ~ 46. If we remove the contribution of the inner disk transit as it may be extremely difficult to detect, the S/N slightly drops to $\simeq 41$.

For estimating the signal to noise ratio, in all cases we have assumed values of w and I appropriate to the $100R_\odot$ star CaII chromospheric emission model of Loeb & Sasselov (1995). These values are unlikely to be pertinent for the fiducial $5R_\odot$ giant star host we are considering, and variations in w and I can affect the detectability significantly.

Figure 7 shows how the transit light curve of our fiducial case changes for different effective widths of the brightened region in the star, while Figure 8 shows how the S/N from the ring transit (i.e. eliminating the disk transit component of the light curve) which we call $(S/N)_{\rm limb}$, varies as a function of this parameter. Notice that in each case we vary I to keep the total flux conserved while keeping the absolute disk intensity fixed. In particular, notice that the S/N is almost constant for very small w and then slowly decreases towards larger values. It is unlikely that for smaller stars the width of the ring will be larger than for our fiducial case, so our S/N could be taken as a lower limit when considering only the dependence on w.

If we vary I, the relative intensity of the ring with respect to the disk, while keeping w and the total flux fixed, $(S/N)_{\rm limb}$ changes as shown in Figure 9 for the narrow band and $S-$value transits. For the latter, the overall S/N drops steadily with the value of I and is effectively zero when $I = 0$, as all signature of the transit is erased from the $S-$value.

We have also assumed for our fiducial case that the transit is equatorial. Figure 10 shows how the S/N varies as a function of the impact parameter b for both narrow band and $S-$value observations. Unlike the case for broad-band transits, the S/N increases with the impact parameter since the planet spends more time crossing the ring. Of course, the

increased duration of the ring transit also means that some of the advantages of using these narrow filters is lost. Figure 7 shows how the transit shape changes with b for our fiducial case, and although for a large range of impact parameters the duration is not significantly altered, for a grazing transit ($b = 1$) the duration is approximately 20 hours.

While thinking of the $S-$value as a photometric index is useful for visualizing the effect, the simplest way to measure this index is from high resolution spectra (e.g. Wright et al. 2004). The advantage of this is that all four channels are observed simultaneously and longer integration times can be achieved. For example, if we observe the fiducial limb brightened transit described before with the HIRES spectrograph (Vogt et al. 1994) at the Keck observatory and measure the $S-$value from the spectrum, we would expect the S/N of the detection to be roughly 77. To calculate this number, we have used the HIRES S/N simulator[7] assuming $1.0''$ seeing and 60 second integrations and keeping all other values to their defaults. The S/N per pixel per observation is 259. Similar observations have been carried out by Shkolnik, Walker & Bohlender (2003) using the Gecko spectrograph (Baudrand & Vitry 2000) at CFHT for studying planet induced chromospheric activity in the F8.5V star HD 179949 by using the variation in the flux of the CaII H and K lines. Also, equivalent width variations smaller than those produced by the limb brightened transits we have discussed here have been detected by Redfield et al. (2008), who studied NaI absorption from HD189733b using using high resolution spectra taken with the HRS spectrograph on the 9.2 meter Hobby-Eberly Telescope. These observations suggest that the effect we have described is currently detectable, provided the intensity in the ring is sufficiently high relative to that of the disk.

5.2. Measuring the Transit Parameters

Accurately measuring transit parameters from the light curve is dependent on an accurate characterization of the star's CaII H & K surface brightness profile. This can be achieved via a priori calculations, which are computationally expensive, or it might be possible to constrain the surface brightness profile from the transit light curve itself with sufficiently large S/N. However, two simple limiting cases can be considered to assess the information content of the ring transit light curves. When $w \ll p$ and when $w > 2p$, it is possible to analytically solve for all the system parameters of immediate interest. For simplicity, we will assume that the orbit of the planet is circular. We argue below that eccentric orbits do not change our argument qualitatively.

[7]http://www.ucolick.org/∼hires/

In general, provided that $a \gg R_*$, it will be valid that

$$P^2 \;=\; \frac{4\pi^2}{GM_*}\, a^3 \;\; \text{(Kepler's Third Law)}, \tag{10}$$

$$t_P \;=\; \frac{PR_*}{\pi a}\, \sqrt{(1-p)^2 - b^2}, \tag{11}$$

where t_P is the time between the end of the first ring transit and the beginning of the second one, or equivalently the time between second and third contact with the photosphere, v_p is the speed of the planet during transit, which we have assumed to be constant, and b is the impact parameter defined as $b = (a/R_*)\cos i$, where i is the orbit's inclination angle. All planetary transits must be confirmed by radial velocity measurements and, in particular, narrow band CaII H and K transits might be easier to observe using high resolution spectra (see §5.1), so we will assume that the radial velocity curve of the system is known. This yields the semi-amplitude of the radial velocity curve, K_*, which is related to the orbital parameters by

$$K_* \;=\; \frac{2\pi a}{P}\, \frac{M_p \sin i}{M_*}, \tag{12}$$

where M_p and M_* are the masses of the planet and the star respectively. Also, from the spectra we should be able to determine the star's surface gravity g,

$$g \;=\; \frac{GM_*}{R_*^2}. \tag{13}$$

In the limit that the width of the limb brightened region is much smaller than the radius of the planet, $w \ll p$, the depth of the ring transit will be given by equation (6)

$$\delta_R \;=\; \frac{p}{\pi}\, \left(\frac{2Iw + \pi p/2}{2Iw + 1} \right),$$

where δ_R is the transit depth when crossing the ring. Also, in this limit, the time duration of one of the ring transits ($t_R/2$) is equal to the ingress time in a typical broad-band transit, so we can state that,

$$\left(\frac{t_P}{t_R + t_P} \right)^2 \;=\; \frac{(1-p)^2 - b^2}{(1+p)^2 - b^2}. \tag{14}$$

In the other limit, when $w > 2p$, if we assume that the intensity in the effective ring is uniform, then we know that the ring transit depth is given by equation (7),

$$\delta_R \;=\; \frac{Ip^2}{Iw(w+2) + 1},$$

and that

$$\frac{t_R}{t_P} \;=\; \frac{\sqrt{(1+w+p)^2 - b^2}}{\sqrt{(1-p)^2 - b^2}} - 1. \tag{15}$$

Note that in both limiting cases we have 6 equations and 7 unknowns (a,M_*,R_*,p,b,M_{pl},w). The easiest parameter to independently estimate is the radius of the star, which can be done with broad-band colors and the calibrations of either Kervella et al. (2004) or van Belle (1999) plus a parallax measurement. Given R_*, the system can now be solved, as we have 6 unknowns and 6 independent equations.

So far we have assumed that the orbit of the planet is perfectly circular in order to simplify the equations. If the orbit was not circular, we must add two more parameters to the system, the eccentricity e and the longitude of periastron ϖ. These two parameters are uniquely determined by the radial velocity curve of the star, adding no more unknowns into our system of equations.

It is unlikely that the true CaII H & K profile of the star will resemble exactly any of these two limits, but it is also unlikely that it will be different enough to qualitatively change the discussion presented here. Thus we conclude that it will be possible to estimate the planetary parameters from a narrow band transit in the same way as with broad-band transits. A proper determination of the typical errors expected in the planetary parameters for a given light curve must be calculated using accurate models of the chromosphere for such stars.

6. Conclusions

Studying planets around giant stars is of interest in understanding and testing theories of planet formation and evolution. Several planets have been found by radial velocity surveys orbiting evolved stars, but to date none have been observed to transit. Using the data compilation of *The Extrasolar Planets Encyclopedia* we have shown that we might reasonably expect that one of the known planets orbiting giant stars to be transiting its host as seen from Earth. Efforts should be made in order to find and observe such an event.

We have also shown that for a typical system with a Jupiter-sized planet and a red giant primary, the nominal S/N per transit is quite large even for a $\sim$ 0.5m telescope. However, once some real-world observational factors are taken into account, these transits may nevertheless be quite difficult to detect. Transit durations are extremely long ($\sim$55 hours for our fiducial system), so in practice only a fraction of the transit would be observable from a single observatory. Even if this is overcome by, for example, observing from several different telescopes around the world, the transit depth is so small that correlated red noise or intrinsic variability could become a dominant factor of the error budget, rendering a definitive detection impossible. It must be kept in mind, however, that very little is known

about the behavior of the red noise and intrinsic variability of red giants on the timescales relevant to this problem.

Several efforts to control the systematic errors in photometric follow-up of transits of bright dwarf stars have been carried out quite successfully, suggesting that similar approaches might yield positive results for transits of giant stars. Also the space transit missions *Kepler* and *COROT* may have the photometric precision needed to detect previously unknown transiting companions to giant stars, provided that a sufficient number of such stars are targeted.

While we argue that detecting broad-band planetary transits in giant stars might be feasible in the near future, we have also described a novel technique to detect these transits by using the CaII H & K chromospheric emission of red giant stars. Because the emission is only produced in the chromosphere, at these wavelengths the light profile of the star looks like a faint disc surrounded by a thin, bright ring, rather than the usual broad-band picture of a limb-darkened disc. Because the light is concentrated in a small region of the star, a transiting planet will produce a more pronounced feature in the star's light curve at these wavelengths.

By approximating the star by a disc surrounded by a brighter ring, we have studied the shape of the transit light curve and the dependence of the S/N on different shapes of the profile. We have shown that, for a typical system, transit depths are well above the red noise amplitude of the current transit surveys searching for planets, and that the S/N of the detection can be very significant, though never as large as the nominal value of the broad-band case. We have shown that for two simple limiting cases, the planet radius, its mass, the impact parameter and the semi-major axis can be inferred when the CaII transit observations are combined with radial velocity observations and an estimation of the star's radius.

Similar observations to those we propose here have been carried out by other authors. These authors have in some cases achieved the precision necessary to detect the ring transit signature of our fiducial case, suggesting that detecting planetary transits of giants through the variations in the CaII H & K lines is feasible with current instrumentation.

The authors would like to thank Jennifer Johnson and Marc Pinsonneault for their help and suggestions, which improved the paper significantly. We would also like to thank Jonathan Fortney for helpful discussions about the effects of stellar irradiation on giant planets, and Birgit Fuhrmeister, Peter Hauschildt, Dimitar Sasselov and Ian Short for discussions about modeling the chromospheres of giant stars. We extend our gratitude to all the students that participated on the discussion of a similar problem in the Order of Magnitude course

taught at The Ohio State University during the Autumn quarter of 2006 from which this work originated. Finally, we would also like to thank the anonymous referee for providing useful comments and suggestions that improved this paper.

REFERENCES

Adelman, S.J. 2001, Baltic Astronomy, 10, 593

Aigrain, S., et al. 2009, A&A, accepted (arXiv:0903.1829)

Alonso, R. et al. 2004, ApJ, 613, L153

Baglin, A., Auvergne, M., Boisnard, L., Lam-Trong, T., Barge, P., Catala, C., Deleuil, M., Michel, E. & Weiss, W. 2006, in COSPAR, Plenary Meeting, 36th COSPAR Scientific Assembly, 36, 3749

Baines, E.K. et al. 2008, ApJ, 680, 728

Baliunas, S.L., Hartmann, L., Vaughan, A.H., Lillier, W. & Dupree, A.K. 1981, ApJ, 246, 473

Baraffe, I., Selsis, F., Chabrier, G., Barman, T. S., Allard, F., Hauschildt, P. H., & Lammer, H. 2004, A&A, 419, L13

Barbieri, M., et al. 2007, A&A, 476, L13

Baudrand, J. & Vitry, R. 2000, Proc. SPIE Vol. 4008, p. 182-193, Optical and IR Telescope Instrumentation and Detectors, eds. Masanori Iye & Alan F. Moorwood

Beatty, T. G., & Gaudi, B. S. 2008, ApJ, 686, 1302

Bodenheimer, P., Laughlin, G., & Lin, D. N. C. 2003, ApJ, 592, 555

Borucki, W.J. et al. 2003, Proc. SPIE, 4854, 129

Burkert, A., & Ida, S. 2007, ApJ, 660, 845

Burrows, A., Guillot, T., Hubbard, W. B., Marley, M. S., Saumon, D., Lunine, J. I., & Sudarsky, D. 2000, ApJ, 534, L97

Burrows, A., Sudarsky, D., & Hubbard, W. B. 2003, ApJ, 594, 545

Burrows, A., Hubeny, I., Budaj, J., & Hubbard, W. B. 2007, ApJ, 661, 502

Butler, R. P., Vogt, S. S., Marcy, G. W., Fischer, D. A., Wright, J. T., Henry, G. W., Laughlin, G., & Lissauer, J. J. 2004, ApJ, 617, 580

Cutri R.M., et al. 2003, University of Massachusetts and Infrared Processing and Analysis Center (IPAC/California Institute of Technology)

de Laverny, P., Mennessier, M.O., Mignard, F. & Mattei, J.A. 1998, A&A, 330, 169

Duncan, D.K., et al. 1991, ApJS, 76, 383

Dupree, A.K., Whitney, B.A. & Pasquini, L. 1999, ApJ, 520, 751

Fischer, D. A., et al. 2007, ApJ, 669, 1336

Fortney, J. J., Marley, M. S., & Barnes, J. W. 2007, ApJ, 659, 1661

Galland, F., Lagrange, A.-M., Udry, S., Chelli, A., Pepe, F., Queloz, D., Beuzit, J.-L., & Mayor, M. 2005, A&A, 443, 337

Galland, F., Lagrange, A.-M., Udry, S., Beuzit, J.-L., Pepe, F., & Mayor, M. 2006, A&A, 452, 709

Gaudi, B. S., Seager, S., & Mallen-Ornelas, G. 2005, ApJ, 623, 472

Gillon, M., et al. 2007, A&A, 472, L13

Gould, A., Dorsher, S., Gaudi, B. S., & Udalski, A. 2006, Acta Astronomica, 56, 1

Guillot, T., & Showman, A. P. 2002, A&A, 385, 156

Guillot, T. 2005, Annual Review of Earth and Planetary Sciences, 33, 493

Hubbard, W. B., Hattori, M. F., Burrows, A., Hubeny, I., & Sudarsky, D. 2007, Icarus, 187, 358

Hauser, M.G., Kelsall, T., Leisawitz, D. & Weiland, J., ed. 1998, *COBE* Diffuse Infrared Background Experiment (DIRBE) Explanatory Supplement, version 2.3 (Greenbelt, MD:GSFC)

Hubbard, W. B., Fortney, J. J., Lunine, J. I., Burrows, A., Sudarsky, D., & Pinto, P. 2001, ApJ, 560, 413

Huelamo, N. et al. 2008, A&Aaccepted (arxiv/0808.2386)

Ida, S., & Lin, D. N. C. 2005, ApJ, 626, 1045

Jackson, B., Greenberg, R., & Barnes, R. 2008, ApJ, 681, 1631

Johnson, J. A., et al. 2007a, ApJ, 665, 785

Johnson, J.A. et al. 2007b, ApJ, 670, 833

Johnson, J.S. et al. 2009, preprint (arXiv:0812.0029)

Kalas, P., et al. 2008, Science, 322, 1345

Kallinger, T., et al. 2008, arXiv:0811.4674

Kennedy, G. M., & Kenyon, S. J. 2008, ApJ, 673, 502

Kervella, P., Thévenin , P., Di Folco, E. & Ségransan E. 2004, A&A, 423, 297

Laughlin, G., Wolf, A., Vanmunster, T., Bodenheimer, P., Fischer, D., Marcy, G., Butler, P., & Vogt, S. 2005, ApJ, 621, 1072

Liu, Y.-J., Sato, B., Zhao, G., & Ando, H. 2009, Research in Astronomy and Astrophysics, Volume 9, Issue 1, pp. 1-4 (2009)., 9, 1

Lissauer, J. J. 1987, Icarus, 69, 249

Loeb, A. & Sasselov, D. 1995, ApJ, 449, L33

Maffei, P. & Tosti, G. 1995, AJ, 109, 2652

Mardling, R. A. 2007, MNRAS, 382, 1768

Marois, C., Macintosh, B., Barman, T., Zuckerman, B., Song, I., Patience, J., Lafrenière, D., & Doyon, R. 2008, Science, 322, 1348

Mayor, M. & Queloz, D. 1995, Nature, 378, 355

Niedzielski, A., Goździewski, K., Wolszczan, A., Konacki, M., Nowak, G., Zieliński 2008, ApJ, accepeted (arxiv/0810.1710)

Nutzman, P. et al. 2008, ApJ, submitted (arxiv/0805.0777)

Pasquini, L., de Medeiros, J.R. & Girardi, L. 2000, A&A, 361, 1011

Pepe, F. et al. 2004, A&A, 423, 385

Pepper, J., Gould, A., & Depoy, D. L. 2003, Acta Astronomica, 53, 213

Perryman, M.A.C. et al. 1997, A&A, 323, 49

Pont, F., Zucker, S. & Queloz, D. 2006, MNRAS, 373,231

Pont, F., et al. 2007, ASP Conference Series, 366, 3

Redfield, S., Endl, M., Cochran, W.D. & Koesterke, L. 2008, ApJ, 673, 87

Setiawan, J. et al. 2003, A&A, 398

Setiawan J. et al. 2008, Proceedings of the ESO/Lisbon/Aveiro Conference, pp. 201-204, Precision Spectroscopy in Astrophysics, Eds. N.C. Santos, L. Pasquini, A.C.M. Correia, and M. Romanielleo

Salasnich, B., Girardi, L., Weiss, A., & Chiosi, C. 2000, A&A, 361, 1023

Sato, B., et al. 2003, ApJ, 597, L157

Sato, B. et al. 2008, PASJ, 60, 539

Seagroves, S. et al. 2003, PASP, 115, 1355

Shkolnik, E., Walker, G.A.H. & Bohlender, D.A. 2003, ApJ, 597, 1092

Showman, A. P., Cooper, C. S., Fortney, J. J., & Marley, M. S. 2008, ApJ, 682, 559

Smak, J. & Wing, R.F. 1979, Acta Astron., 29, 199

Smith, B.J., Leisawitz, D., Castelaz, M.W. & Luttermoser, D. 2002, AJ, 123, 948

Torres, G., Winn, J. N., & Holman, M. J. 2008, ApJ, 677, 1324

Udalski, A., Kubiak, M. & Szymański, M. 1997, Acta Astron., 47, 319

van Belle, G. 1999, PASP, 111, 1515

van Belle, G. & von Braun, K. 2009, ApJ, accepted (arXiv:0901.1206)

Vaughan, A.H., Preston, G.W. & Wilson, O.C. 1978, PASP, 90, 267

Vogt, S.S. et al. 1994, Proc. SPIE Instrumentation in Astronomy VIII, eds. David L. Crawford & Eric R. Craine, Volume 2198, p.362

Wilson, O.C. 1978, ApJ, 226, 379

Winn, J. N., & Holman, M. J. 2005, ApJ, 628, L159

Winn, J., Holman, M.J. & Roussanova, A. 2007, ApJ, 657, 1098

Winn, J. et al.] 2009, AJ, in press (arXiv:0901.4346)

Woźniak, P.R., McGowan, K.E. & Vestrand, W.T. 2004, ApJ, 610, 1038

Wright, J.T., Marcy, G.W., Butler, R.P. & S.S. Vogt 2004, ApJ, 152, 261

Yee, J. C., & Gaudi, B. S. 2008, ApJ, 688, 616

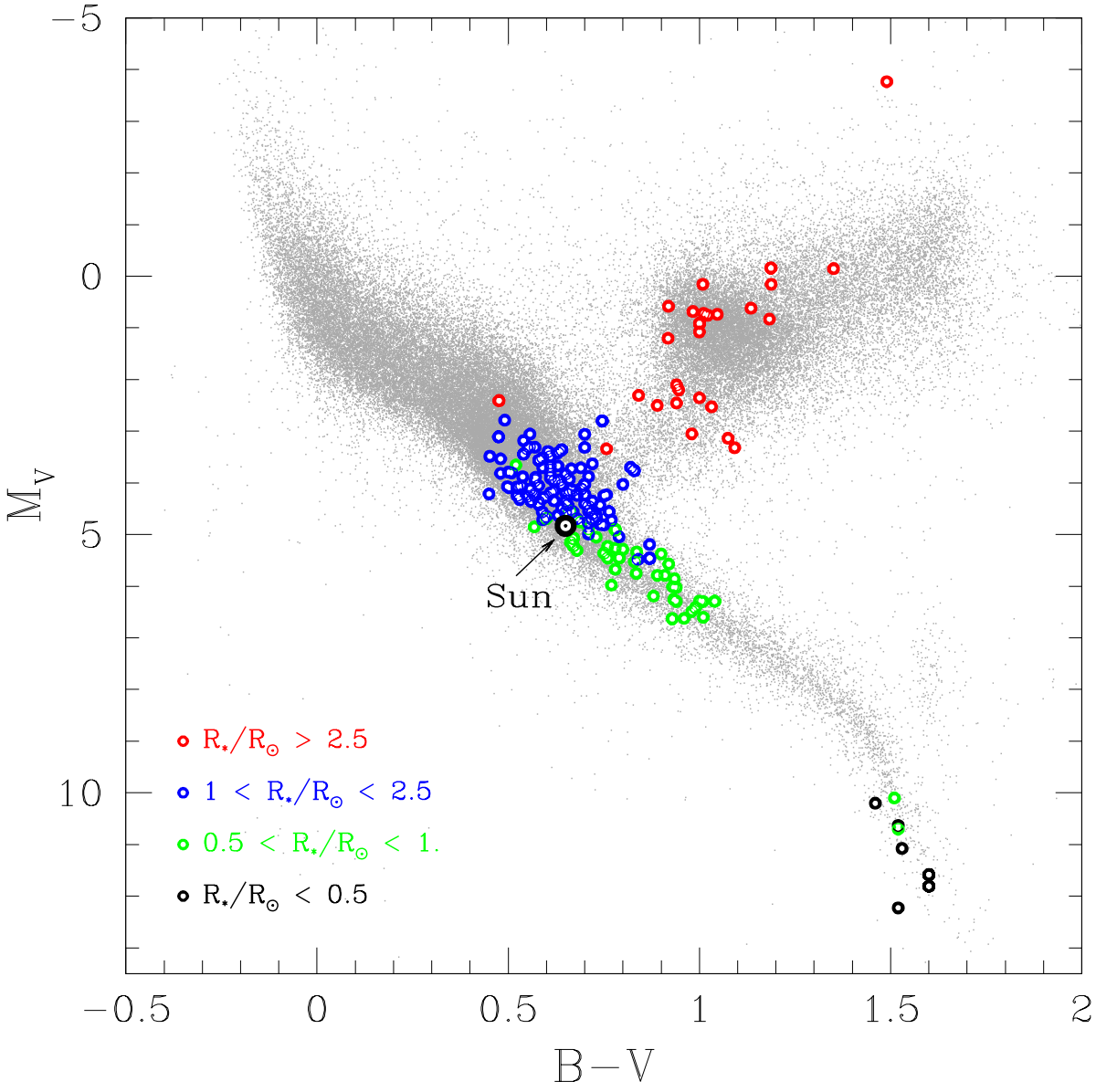

Fig. 1.— Color-magnitude diagram of the stars that were found by RV surveys to host exoplanets (*solid circles*). Stars are color coded by their radius: $R_* < 0.5R_\odot$ (*black*), $0.5 < R_* < 1.R_\odot$ (*green*), $1. < R_* < 2.5R_\odot$ (*blue*) and $R_* > 2.5R_\odot$ (*red*). When a value for the radius was not listed by *The Extrasolar Planets Encyclopedia* we estimated it from the van Belle (1999) color–angular size relations combined with the Hipparcos mission parallax measurements. For reference, we also show all the Hipparcos sources (*grey dots*).

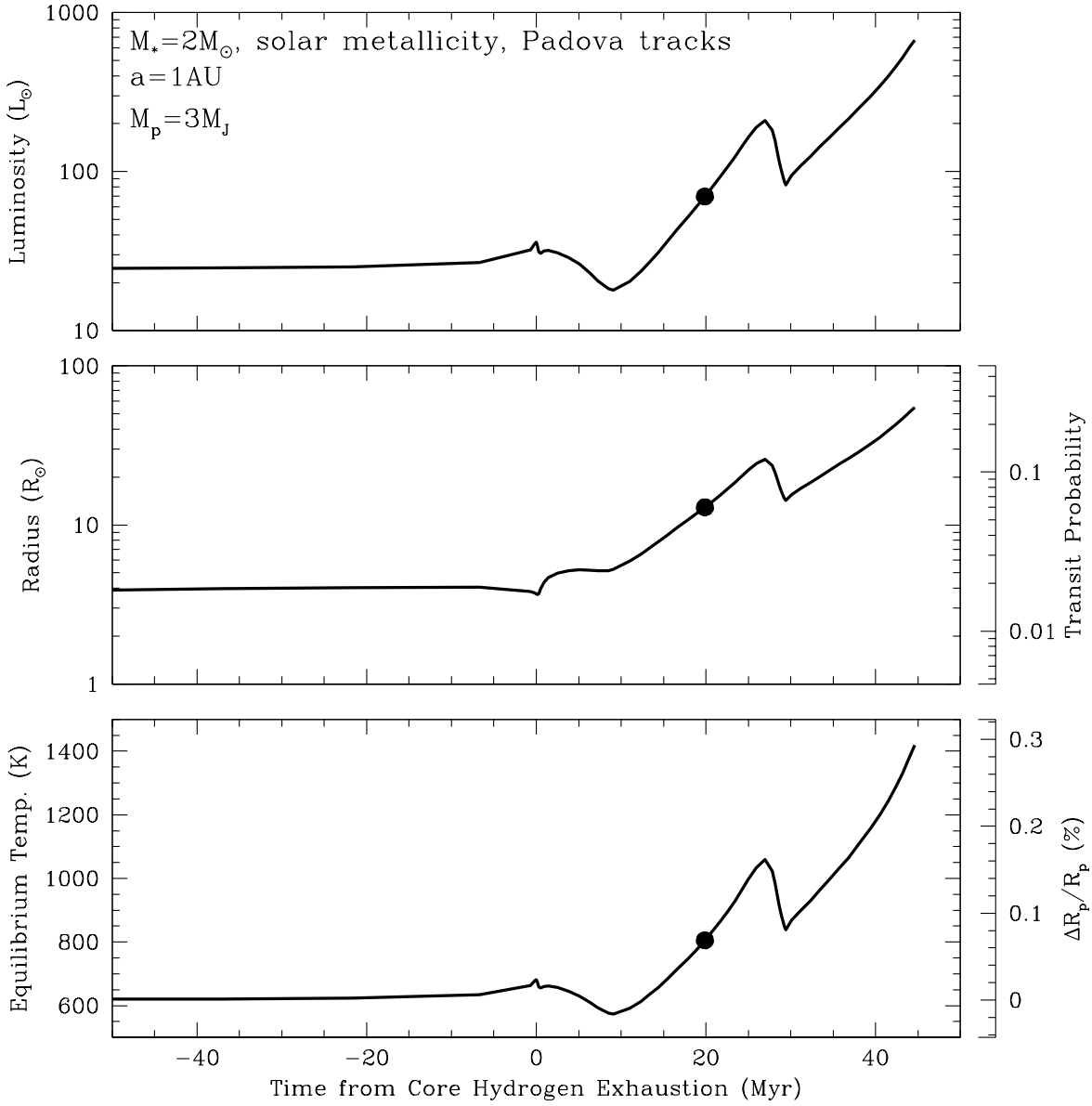

Fig. 2.— Evolution of a $2M_\odot$ star as a function of time in Myr relative to the time when the hydrogen in its core is exhausted, i.e. the end of its main-sequence lifetime, from the evolutionary tracks of Salasnich et al. (2000). Top Panel: Luminosity as a function of time. Middle Panel: Radius as a function of time. The extreme right axis shows the transit probability as a function of time for a planet at $a = 1$ AU. Bottom Panel: The evolution of the equilibrium temperature of a planet at 1 AU as a function of time. Here we have assumed an albedo of $A_B = 0$ and complete redistribution of heat. The extreme right axis shows the corresponding change in the radius of a planet with $M_p = 3\ M_J$, relative to its radius when the host is on the main-sequence. In all three panels, the dot shows the parameters of a star with a post-main sequence age of ~ 20 Myr: $L \simeq 70\ L_\odot$, $R_* \simeq 14 R_\odot$, and $T_{eq} \simeq 800$ K. The stellar and planetary parameters of this system approximates those of the known planet/star system HD 173416 (Liu et al. 2009).

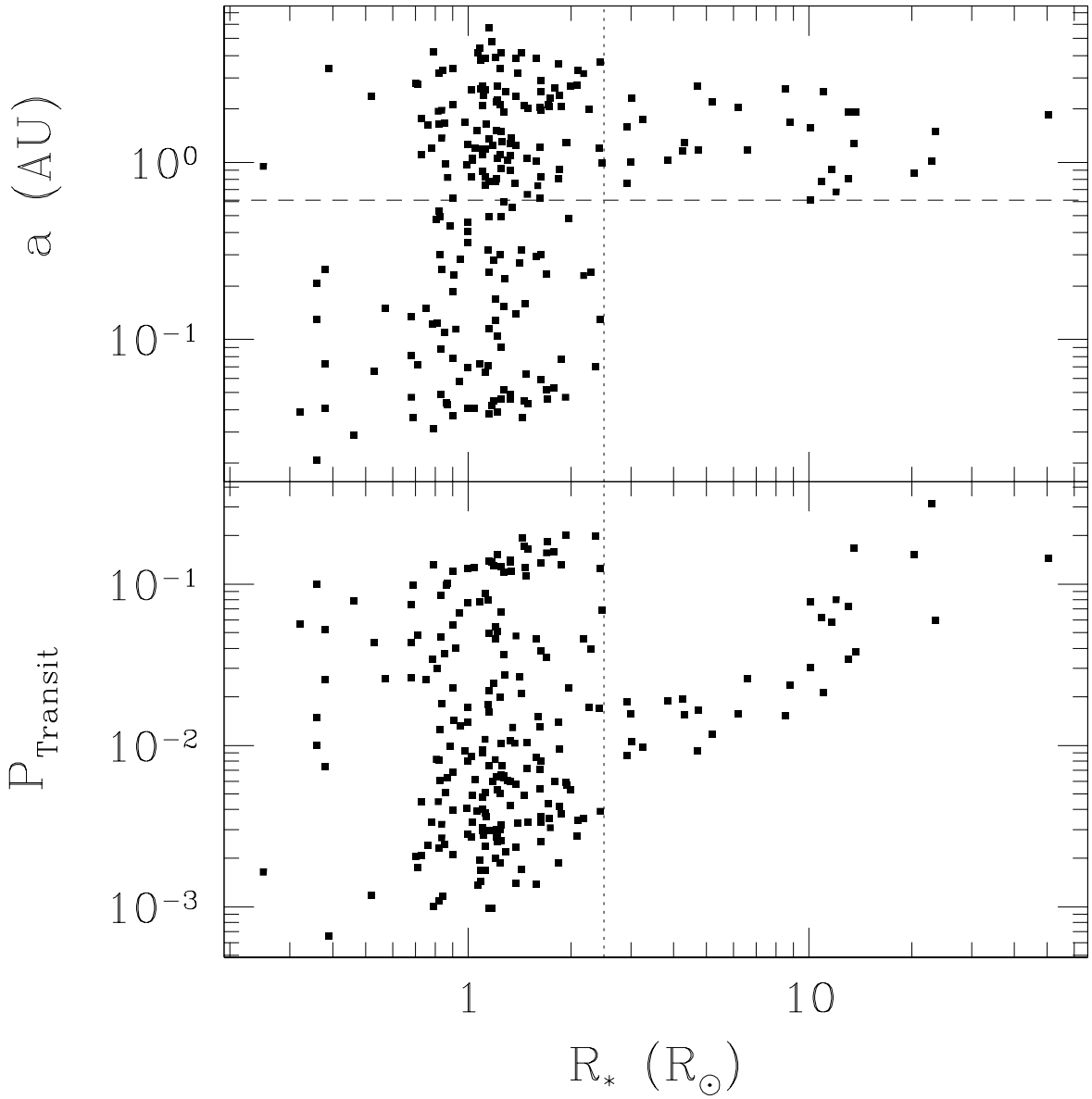

Fig. 3.— Semi-major axis (*top*) and transit probability (*bottom*) as a function of stellar radius for stars with exoplanets detected by RV, as culled from *The Extrasolar Planets Encyclopedia*. The dashed line in the top panel shows the minimum semi-major axis for planets around giant stars determined by Sato et al. (2008). The vertical dotted line indicates our adopted radius cut of $2.5R_\odot$ for selecting giant stars.Note that our sample is composed 29 planets orbiting the 27 giant stars shown on Figure 1. The two multiple planetary systems correspond to HD102272 and HD60532.

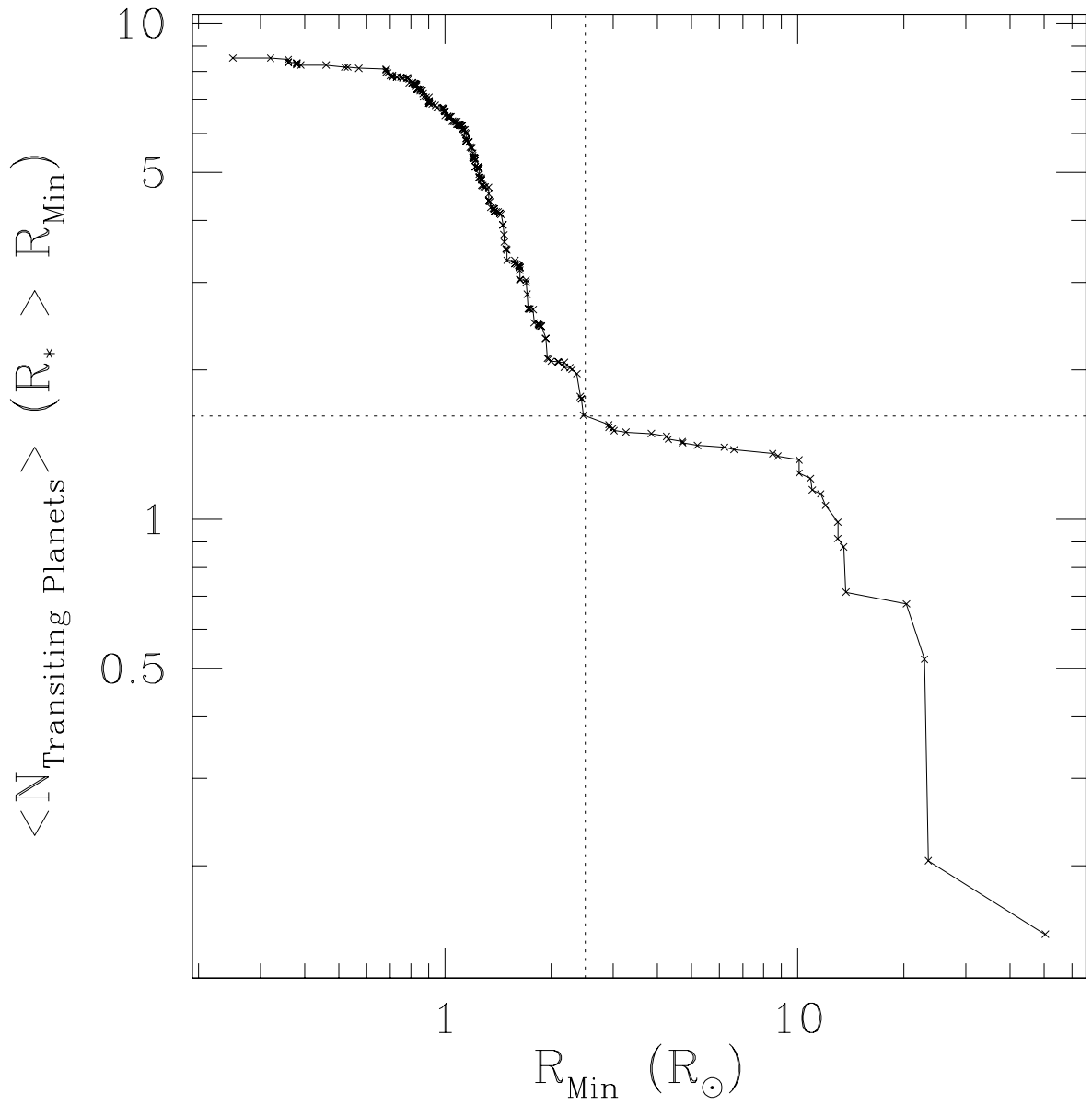

Fig. 4.— Expected number of transiting planets as a function of the minimum radius of the host star for exoplanets found by RV surveys. Each cross shows expected number of transiting systems, calculated by successively eliminating the smallest host star from total sample of RV-detected exoplanets culled from the *The Extrasolar Planets Encyclopedia* list. The vertical dashed line shows our adopted radius cut of $2.5R_\odot$ for giant stars, while the horizontal dashed line shows the expected number of transiting planets orbiting hosts stars above this radius threshold linearly interpolated between the two adjacent points.

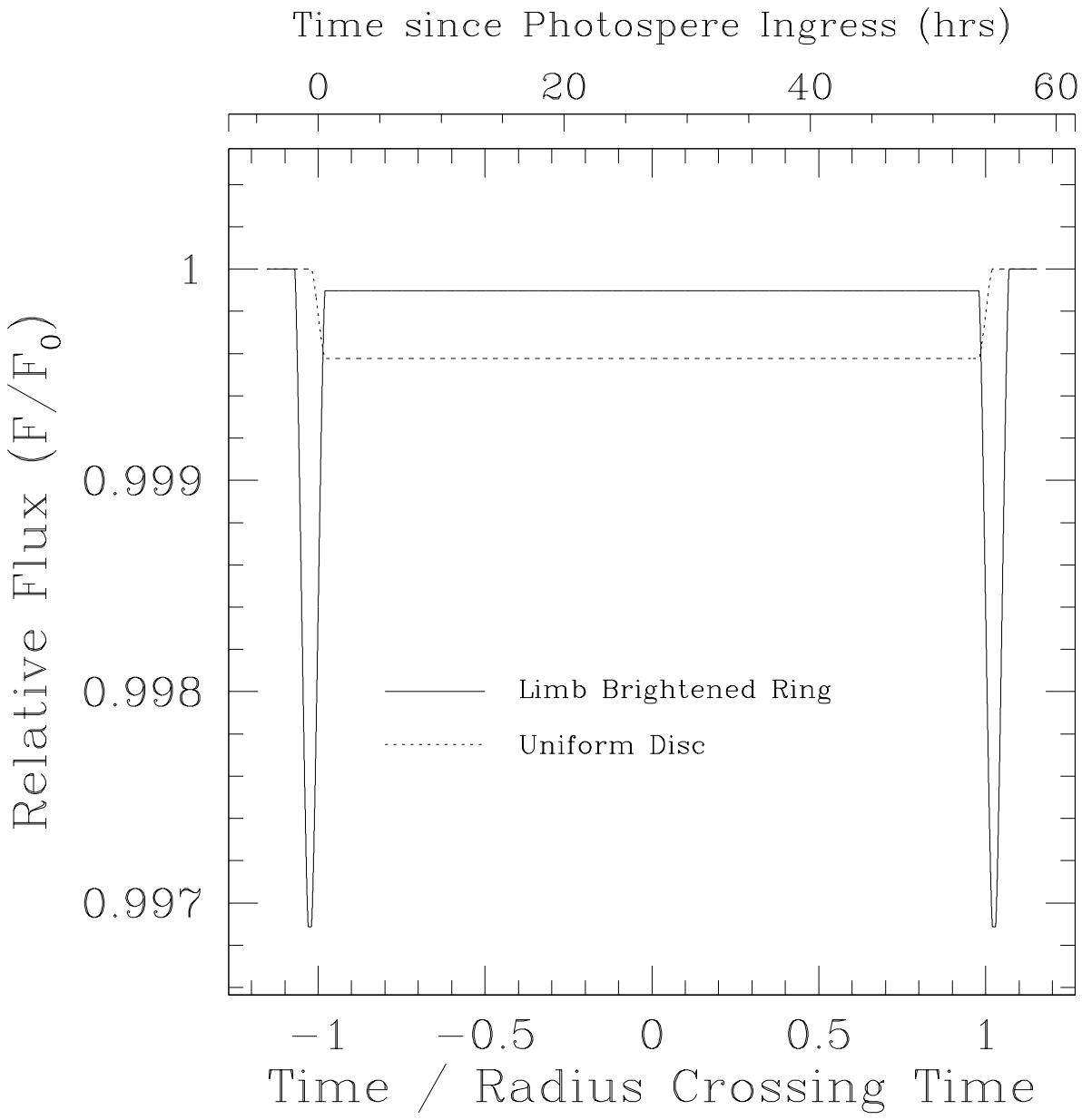

Fig. 5.— The solid line shows the light curve of a Jupiter-sized planet transiting a $5R_{\odot}$ giant star, as observed through narrow bands centered in the core of the CaII H and K lines. We have assumed a central transit. The dashed line shows the transit light curve for the same system but assuming a uniform surface brightness distribution, as would be observed through broad-band filters. For the narrow band observations, we have modeled the star as an inner disk surrounded by a ring of uniform brightness with an intensity 30 times larger than the inner disk. The width of the ring is 5% of the radius of the star.

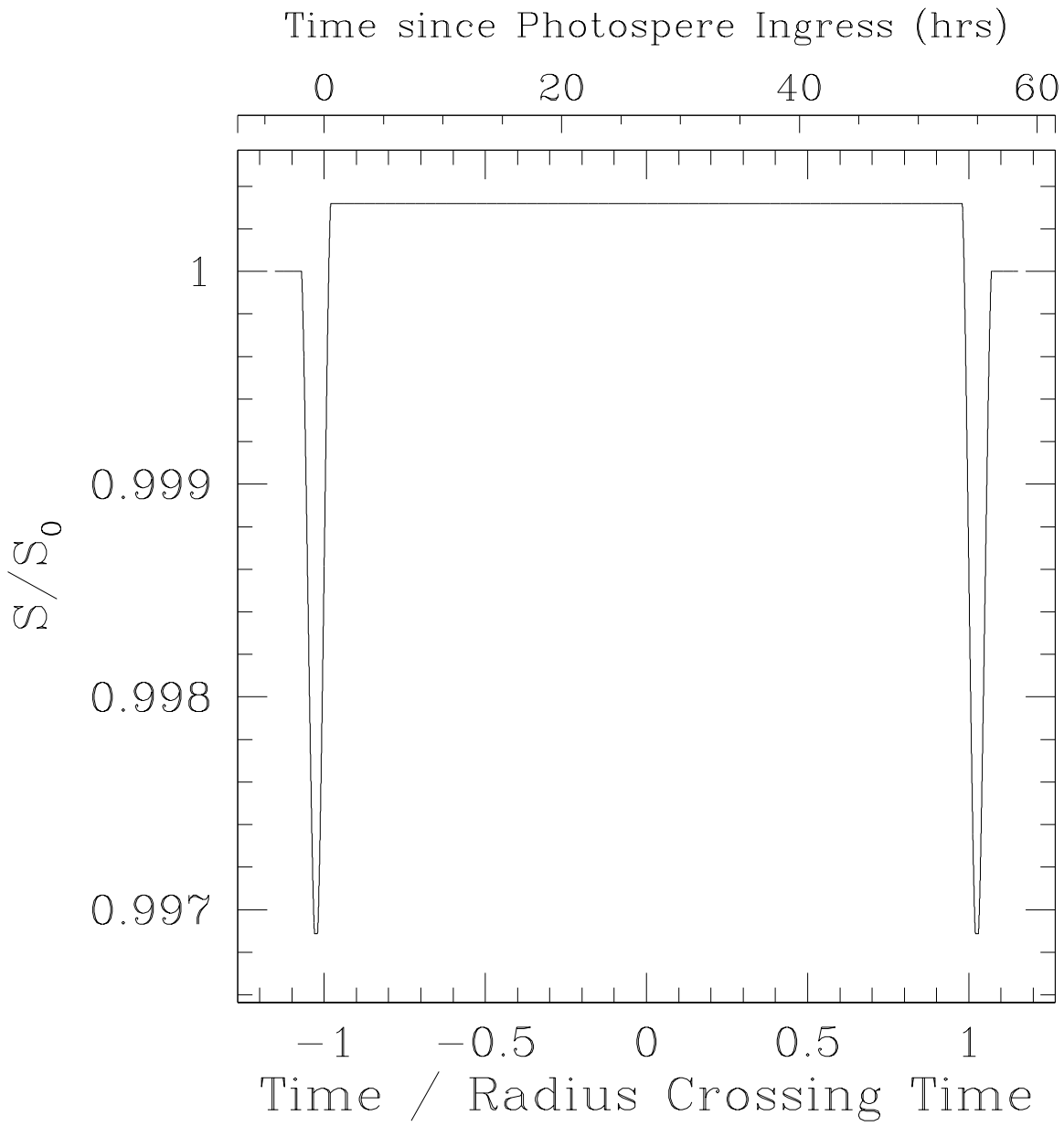

Fig. 6.— The light curve of a Jupiter-sized planet transiting a $5R_{\odot}$ giant star, as observed through the Mount Wilson $S-$value. The parameters for the system are described in the text and are the same as for Figure 5.

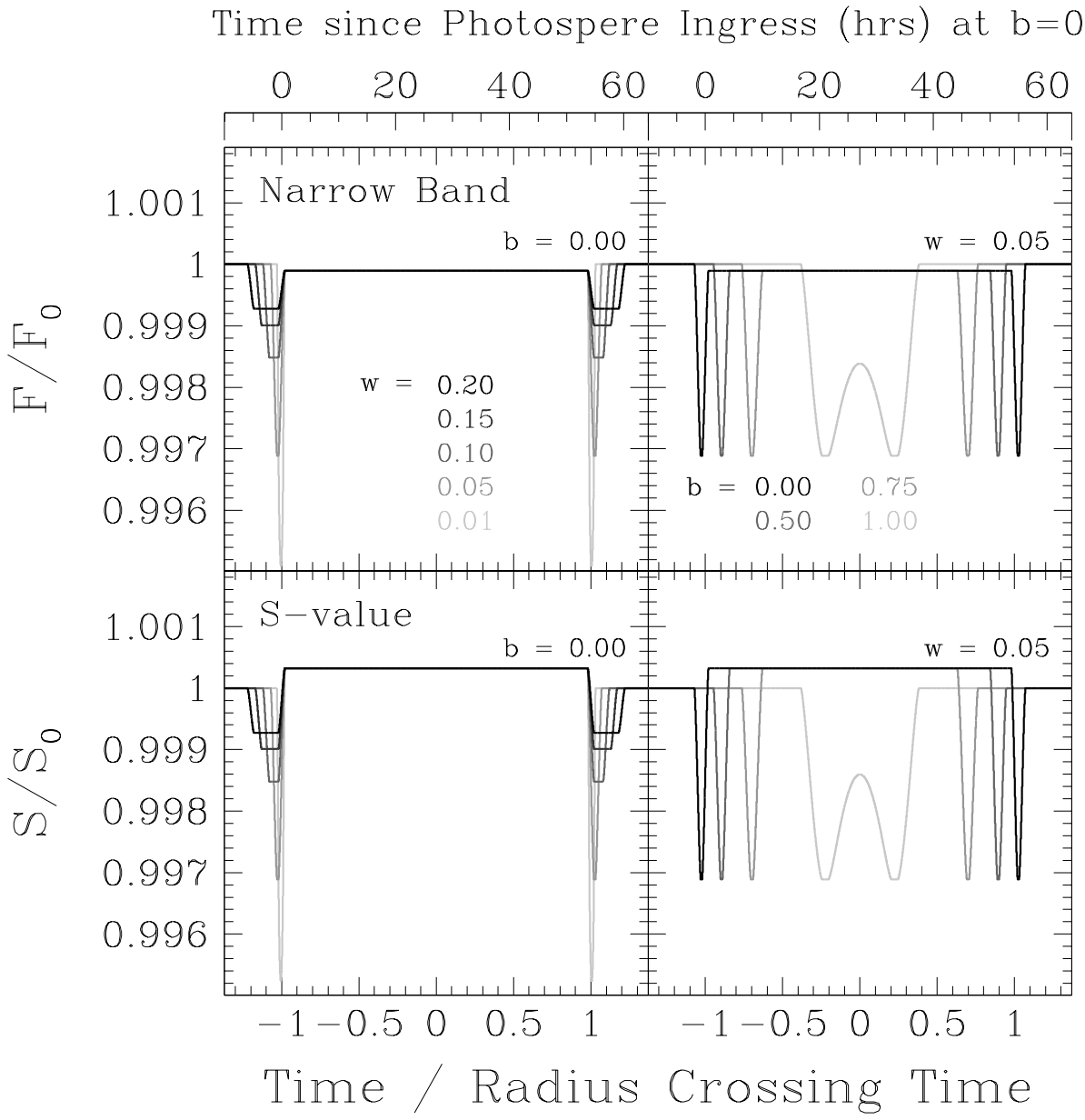

Fig. 7.— Transit light curves of our fiducial case for different values of the width of the brightened ring w (*left*) and the impact parameter b (*right*) as viewed through the H & K narrow bands (*top*) and the Mount Wilson $S-$value (*bottom*). Notice that when w is changed, I is adjusted to conserve the stellar flux.

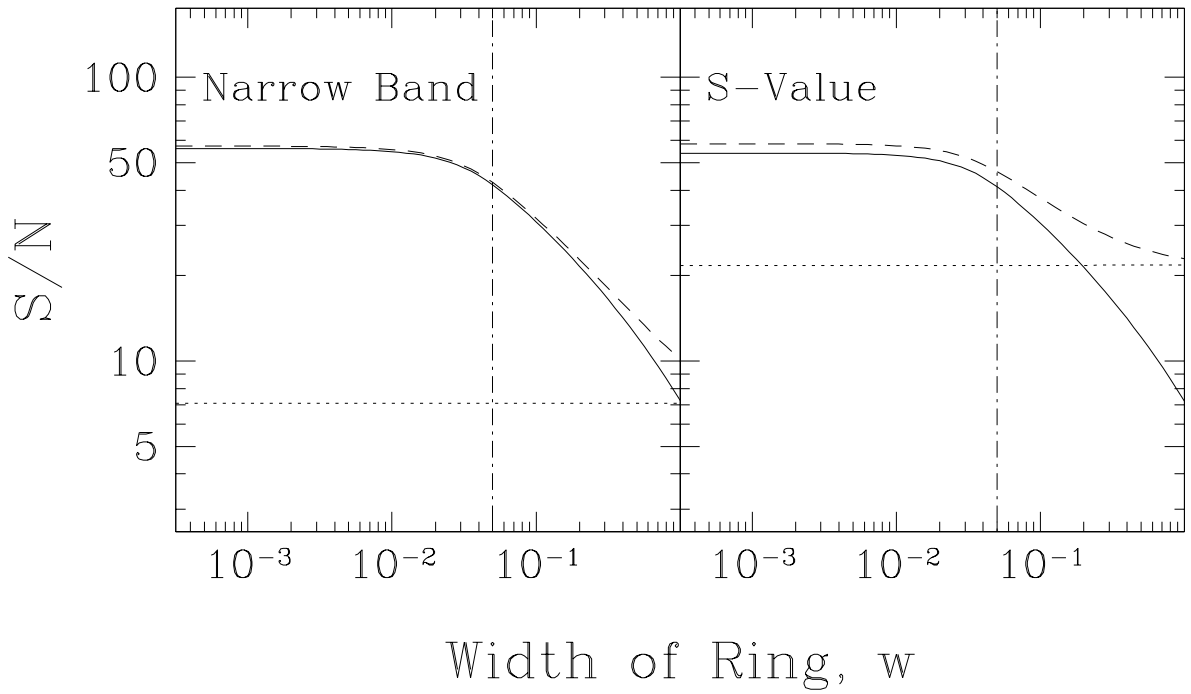

Fig. 8.— The solid line shows $(S/N)_{limb}$, the S/N of only the ring portion of the transit, as a function of the width of the ring in units of the star's radius, as observed through the H and K narrow bands (*left*), and the Mount Wilson $S-$value (*right*). The dashed lines show the behavior of the total S/N (ring plus disk) while the dotted lines show the S/N of only the disk portion of the transit. The dot-dashed line shows the value of w we chose for the fiducial case analyzed in detail in the text.

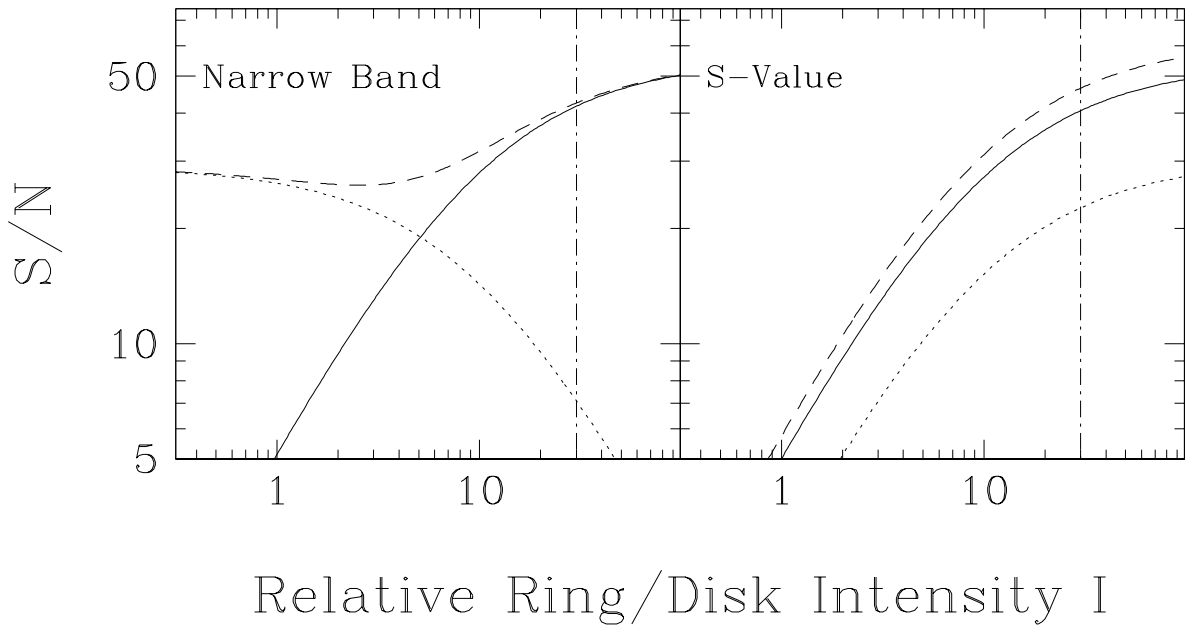

Fig. 9.— The solid line shows $(S/N)_{limb}$, the S/N of the only the ring part of the transit, as a function of the relative intensity of the ring compared to the inner disk, I, as observed through the H and K narrow bands (*left*), and the Mount Wilson $S-$value (*right*). The dashed lines show the behavior of the total S/N (ring plus disk) while the dotted lines show the S/N of only the disk part of the transit. The dot-dashed line shows the value of I we chose for the fiducial case analyzed in the text. Note that when $I = 0$, the $S-$value is constant through out the transit.

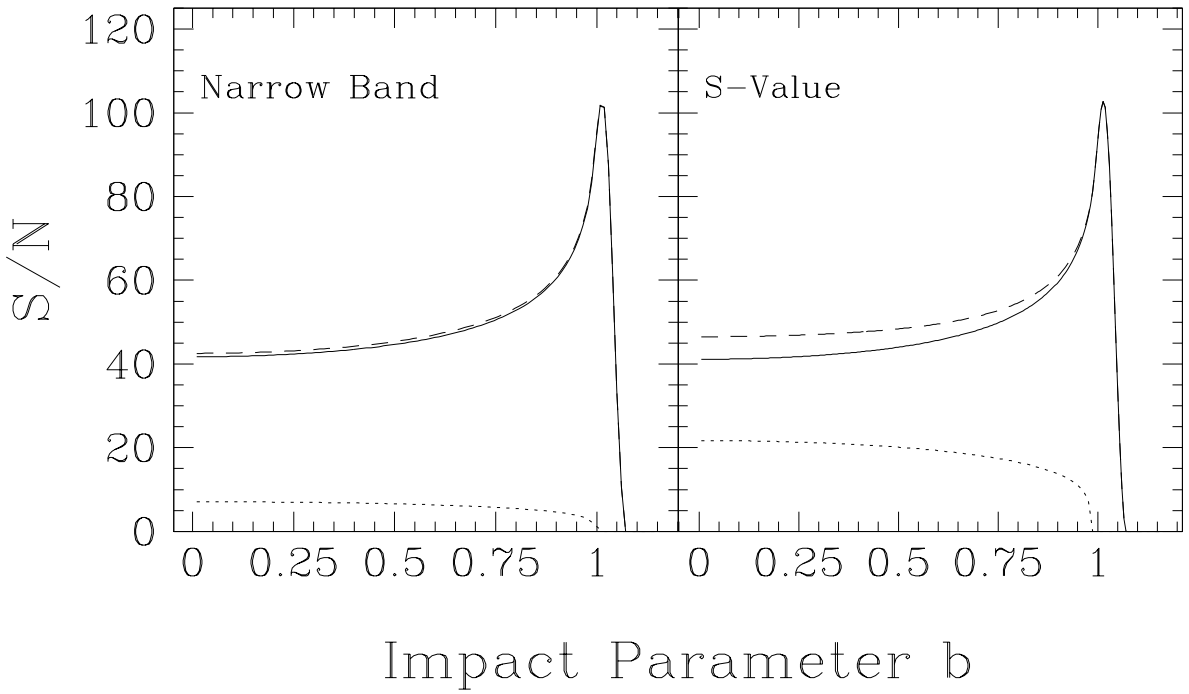

Fig. 10.— The solid line shows $(S/N)_{limb}$, the S/N of only the ring part of the transit, as a function of the impact parameter in units if the star radius, b, as observed through the H and K narrow bands (*left*), and the Mount Wilson $S-$value (*right*). The dashed lines show the behavior of the total S/N (ring plus disk) while the dotted lines show the S/N of only the disk part of the transit. Note that, contrary to broad-band transits, the S/N of the detection increases as a function of b, as the planet spends more time transiting the limb brightened ring of the star.